

This is an Open Access document downloaded from ORCA, Cardiff University's institutional repository: <https://orca.cardiff.ac.uk/id/eprint/144575/>

This is the author's version of a work that was submitted to / accepted for publication.

Citation for final published version:

Jia, Zhiyong, Rondiya, Sachin R., Cross, Russell W., Wang, Cheng, Dzade, Nelson Y. and Zhang, Chuang 2021. Highly active methanol oxidation electrocatalyst based on 2D NiO porous nanosheets: a combined computational and experimental study. *Electrochimica Acta* 394 , 139143. 10.1016/j.electacta.2021.139143

Publishers page: <http://dx.doi.org/10.1016/j.electacta.2021.139143>

Please note:

Changes made as a result of publishing processes such as copy-editing, formatting and page numbers may not be reflected in this version. For the definitive version of this publication, please refer to the published source. You are advised to consult the publisher's version if you wish to cite this paper.

This version is being made available in accordance with publisher policies. See <http://orca.cf.ac.uk/policies.html> for usage policies. Copyright and moral rights for publications made available in ORCA are retained by the copyright holders.



# **Highly Active Methanol Oxidation Electrocatalyst based on 2D NiO Porous Nanosheets: A Combined Computational and Experimental Study**

ZhiyongJia<sup>a</sup>; Sachin R. Rondiya<sup>b</sup>; Russell W. Cross<sup>b</sup>; Cheng Wang <sup>c</sup>; Nelson Y. Dzade<sup>b\*</sup>;

Chuang Zhang<sup>a,c\*</sup>

<sup>a</sup> School of Automobile and Traffic Engineering, Hubei University of Arts and Science, Xiangyang 441058,  
P. R. China.

<sup>b</sup>School of Chemistry, Cardiff University, Main Building, Park Place, Cardiff, CF103AT, Wales, United  
Kingdom.

<sup>c</sup> Zhang Jiagang Joint Institute for Hydrogen Energy and Lithium-Ion Battery Technology, INET, Tsinghua  
University, Beijing 100000, P. R. China.

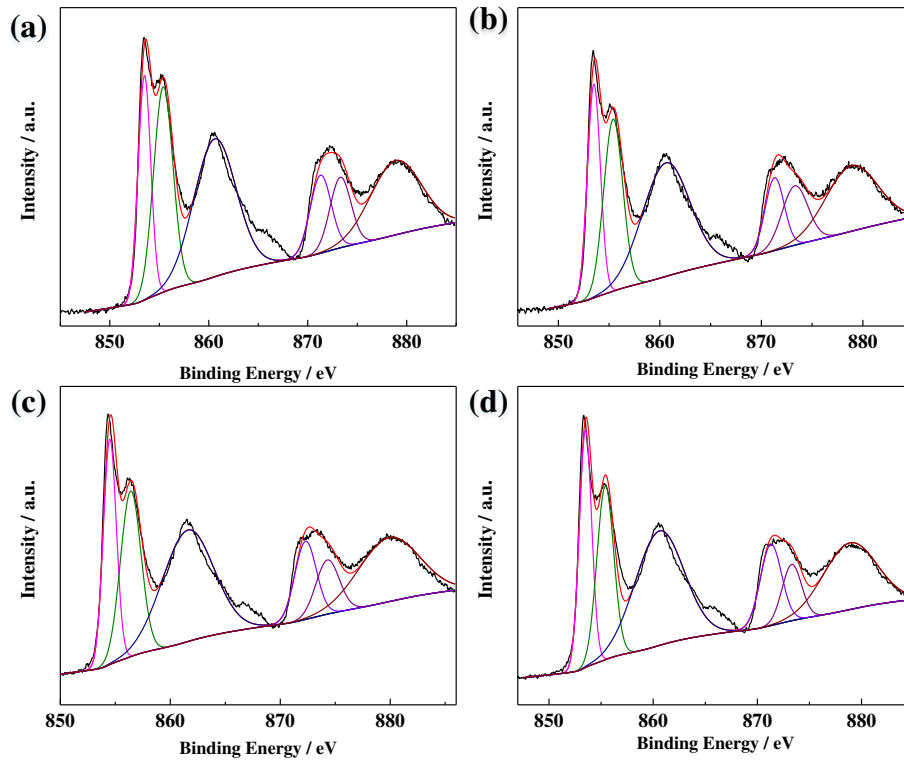


Fig.S1: Ni 2pXPS spectra of the 350-NiO (a), 450-NiO (b), 550-NiO (c) and 650-NiO.

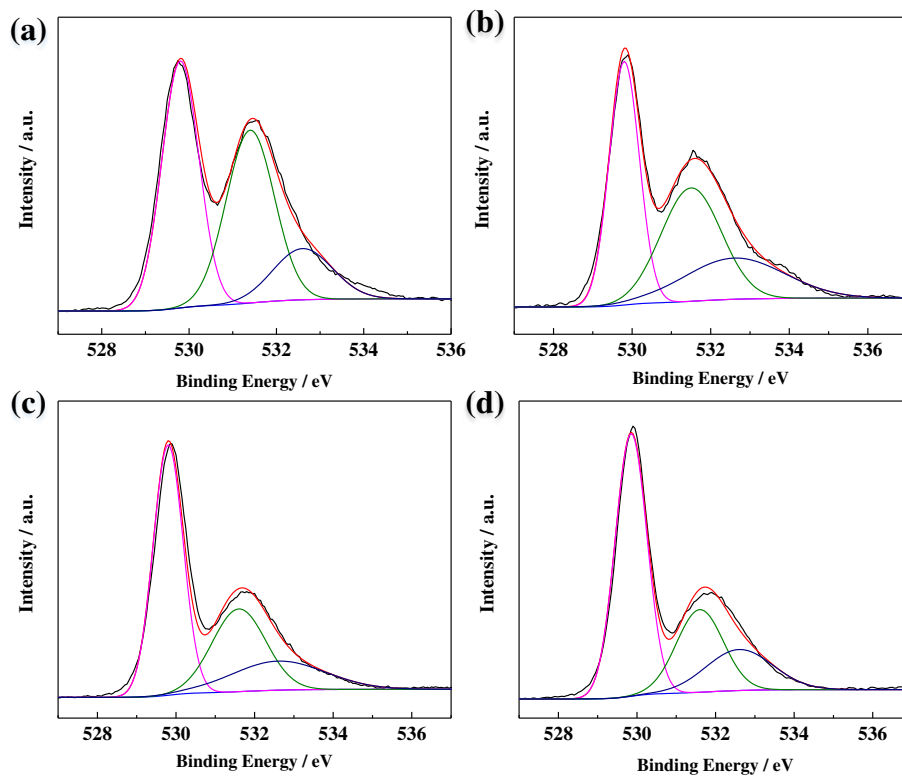


Fig.S2:O 1sXPS spectra of 350-NiO (a), 450-NiO (b), 550-NiO (c) and650-NiO.

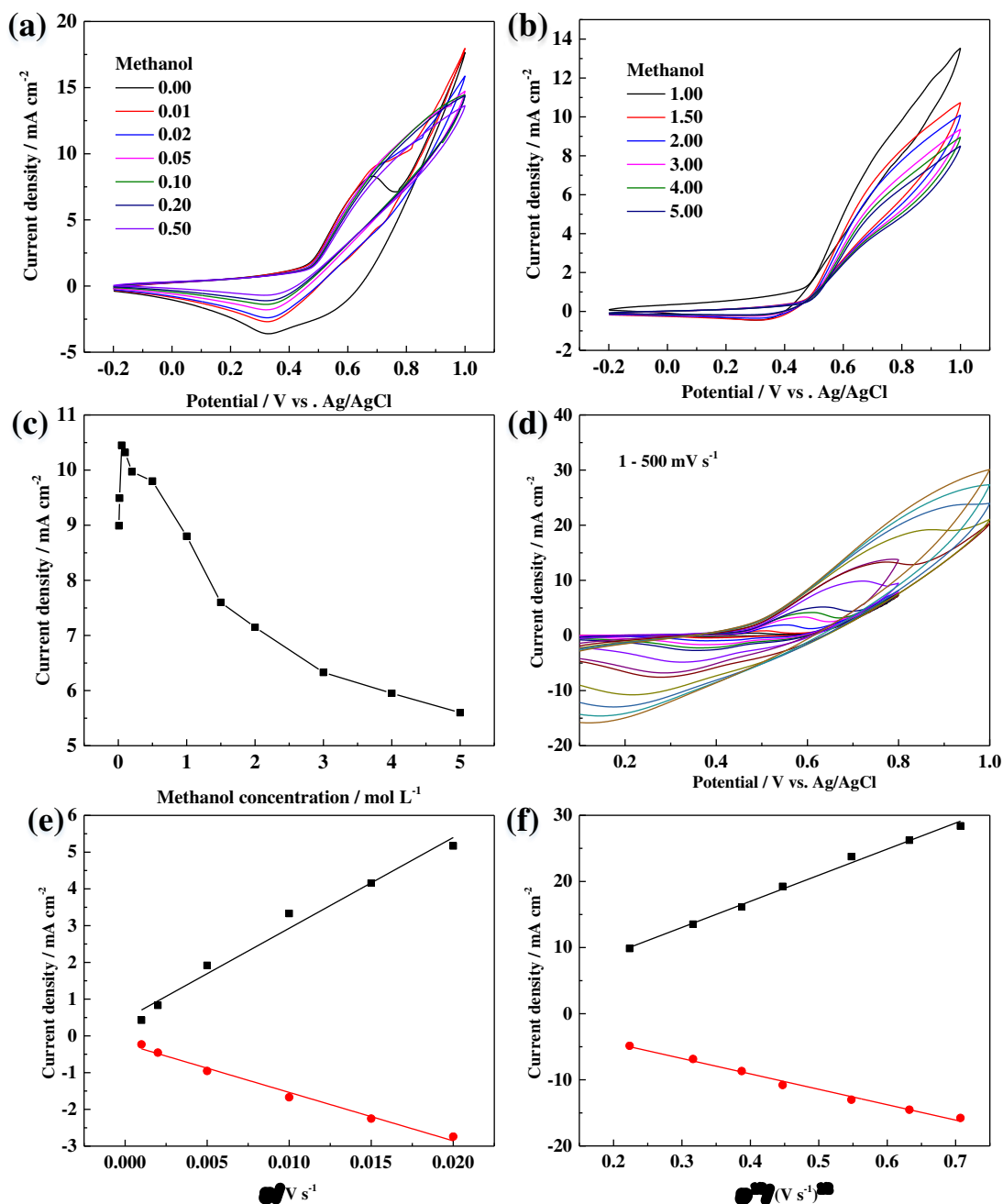


Fig.S3:350-NiO. (a) and (b) CV curves under different methanol concentration at  $50 \text{ mV s}^{-1}$ , (c) comparison of oxidation peaks of methanol at different concentrations; (d) CV curves at different scan rates (1, 2, 5, 10, 15, 20, 50, 100, 150, 200, 300, 400, 500), (e) relationship of current densities of oxidation and reduction peaks at low sweep speed (1, 2, 5, 10, 15 and 20  $\text{mV s}^{-1}$ ), (f) relationship of current densities of oxidation and reduction peaks at higher sweep speed (50, 100, 150, 200, 300, 400 and 500  $\text{mV s}^{-1}$ ); under the 0.1 M KOH solution in the  $N_2$ -saturated.

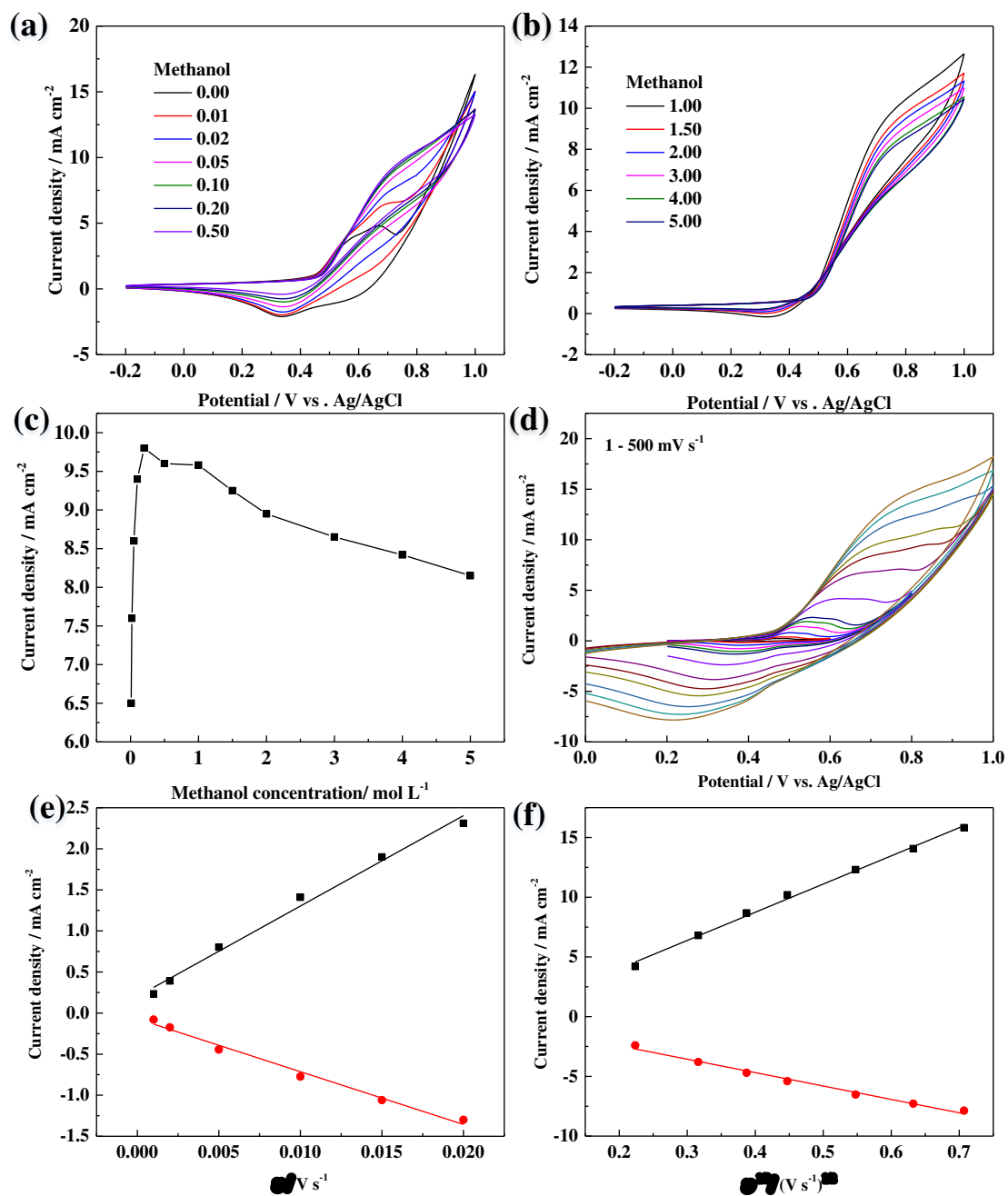


Fig.S4:450-NiO. (a) and (b) CV curves under different methanol concentration at  $50 \text{ mV s}^{-1}$ , (c) comparison of oxidation peaks of methanol at different concentrations; (d) CV curves at different scan rates (1, 2, 5, 10, 15, 20, 50, 100, 150, 200, 300, 400, 500), (e) relationship of current densities of oxidation and reduction peaks at low sweep speed (1, 2, 5, 10, 15 and 20  $\text{mV s}^{-1}$ ), (f) relationship of current densities of oxidation and reduction peaks at higher sweep speed (50, 100, 150, 200, 300, 400 and 500  $\text{mV s}^{-1}$ ); under the 0.1 M KOH solution in the  $\text{N}_2$ -saturated.

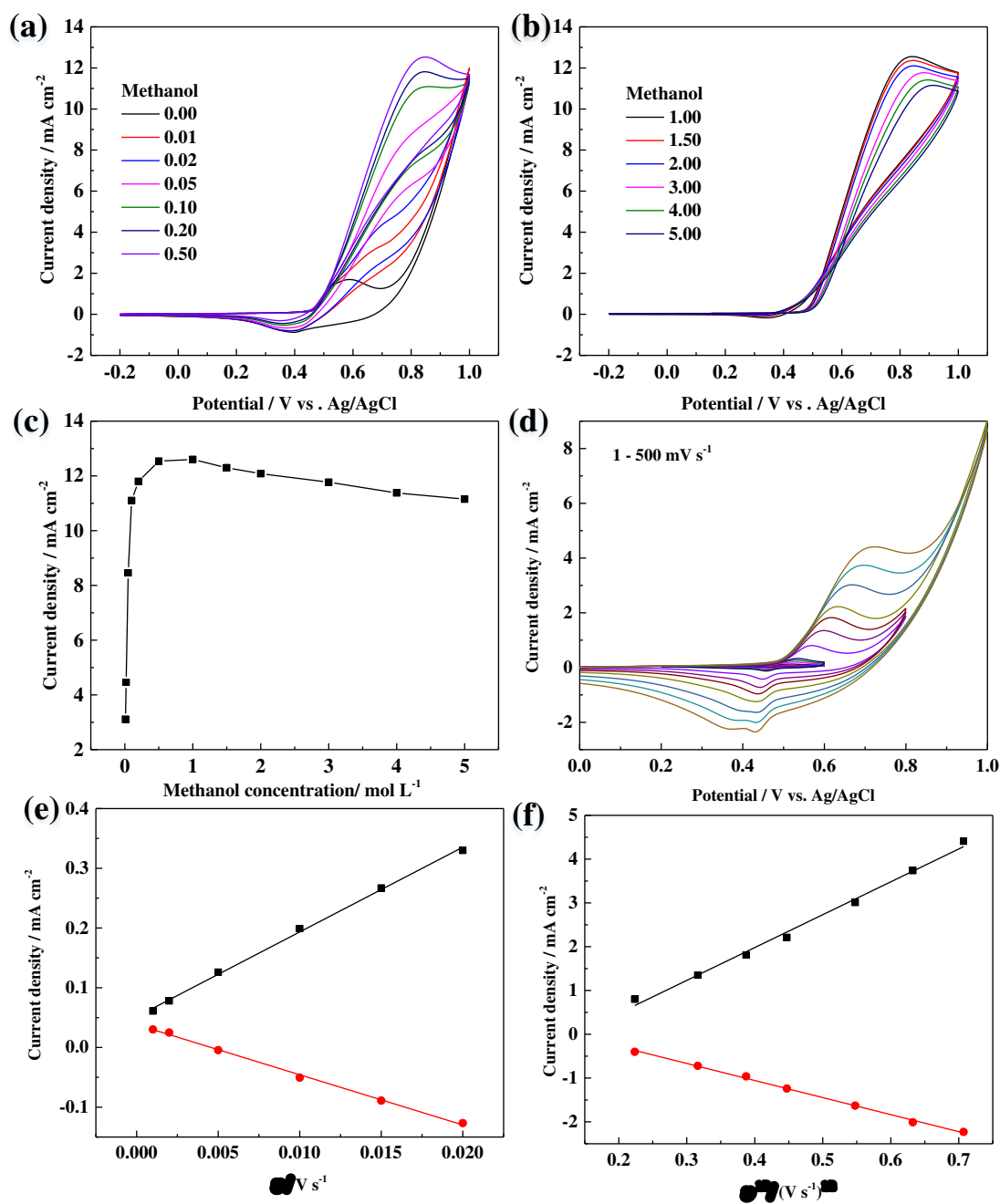


Fig.S5:550-NiO. (a) and (b) CV curves under different methanol concentration at 50 mV s<sup>-1</sup>, (c) comparison of oxidation peaks of methanol at different concentrations; (d) CV curves at different scan rates (1, 2, 5, 10, 15, 20, 50, 100, 150, 200, 300, 400, 500), (e) relationship of current densities of oxidation and reduction peaks at low sweep speed (1, 2, 5, 10, 15 and 20 mV s<sup>-1</sup>), (f) relationship of current densities of oxidation and reduction peaks at higher sweep speed (50, 100, 150, 200, 300, 400 and 500 mV s<sup>-1</sup>); under the 0.1 M KOH solution in the N<sub>2</sub>-saturated.

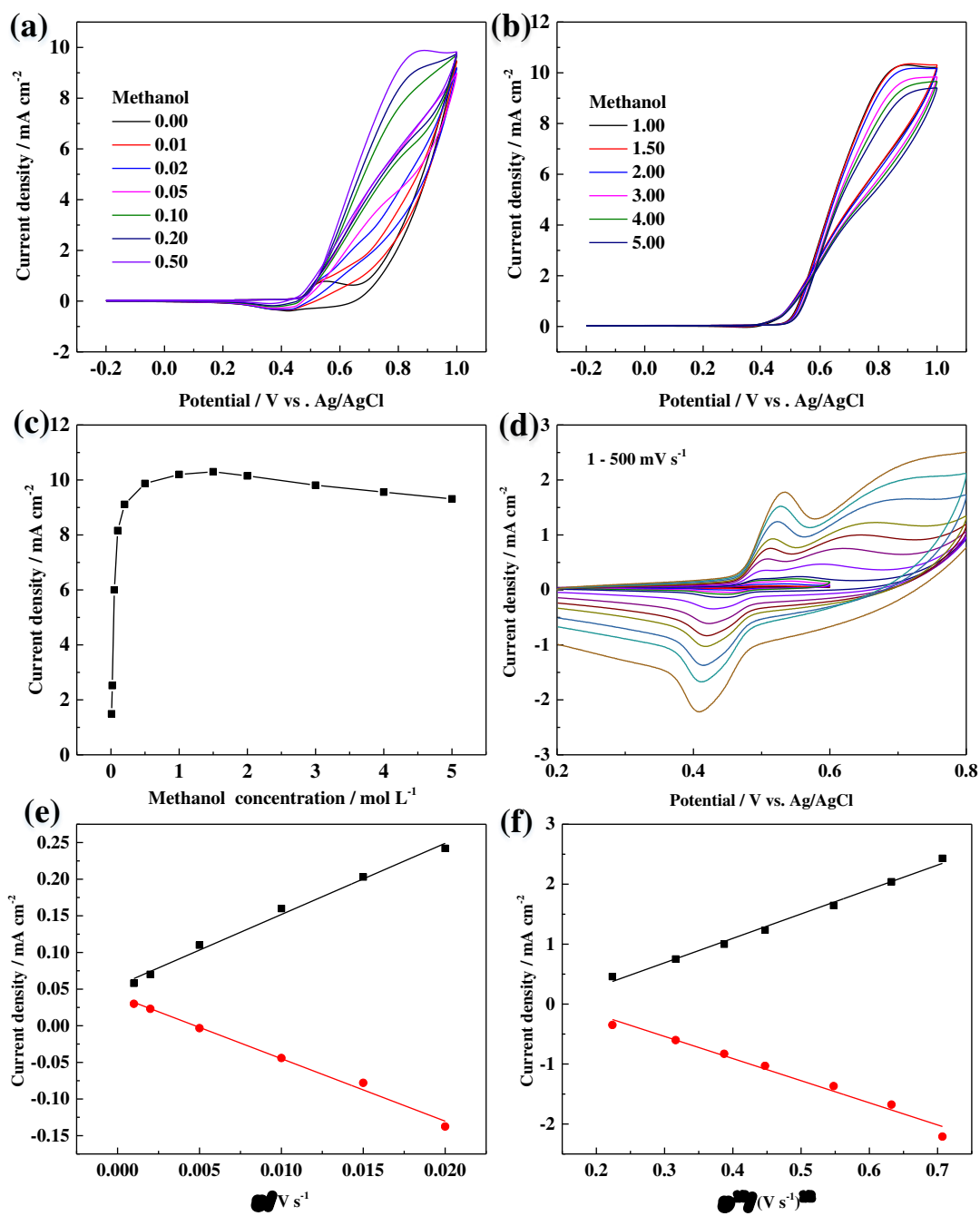


Fig.S6:650-NiO. (a) and (b) CV curves under different methanol concentration at  $50 \text{ mV s}^{-1}$ , (c) comparison of oxidation peaks of methanol at different concentrations; (d) CV curves at different scan rates (1, 2, 5, 10, 15, 20, 50, 100, 150, 200, 300, 400, 500), (e) relationship of current densities of oxidation and reduction peaks at low sweep speed (1, 2, 5, 10, 15 and 20  $\text{mV s}^{-1}$ ), (f) relationship of current densities of oxidation and reduction peaks at higher sweep speed (50, 100, 150, 200, 300, 400 and 500  $\text{mV s}^{-1}$ ); under the 0.1 M KOH solution in the  $\text{N}_2$ -saturated.



Table S1: Adsorption sites, configurations, energies, and structural parameters for intermediates involved in CH<sub>3</sub>OH oxidation on NiO(100).

species	site	configurations	E <sub>ads</sub> (eV)	d <sub>C-O</sub> (Å)	d <sub>Ni-O</sub> (Å)	d <sub>Ni-C</sub> (Å)
CH <sub>3</sub> OH	Ni-top	η <sup>1</sup> (O)	-2.14	1.447	2.011	
CH <sub>3</sub> O	Ni-top	η <sup>1</sup> (O)	-2.42	1.411	1.744	
CH <sub>2</sub> OH	Ni <sub>2</sub> -top	η <sup>2</sup> (C, O)	-2.25	1.456	2.019	1.937
CH <sub>2</sub> O	Ni <sub>2</sub> -top	η <sup>2</sup> (C, O)	-1.70	1.326	1.836	1.978
CHO	Ni <sub>2</sub> -top	η <sup>2</sup> (C, O)	-3.79	1.251	1.870	1.809
CO	Ni <sub>2</sub> -bridge	η <sup>1</sup> (C)	-4.20	1.176		1.867, 1.734
HCOOH	Ni <sub>2</sub> -top	η <sup>3</sup> (C, O, O)	-2.85	1.266, 1.402	1.889, 2.075	2.122
COOH	Ni <sub>2</sub> -top	η <sup>2</sup> (C, O)	-2.33	1.268, 1.334	1.908	1.851
HCOO	Ni <sub>2</sub> -top	η <sup>2</sup> (O, O)	-1.88	1.270, 1.275	1.869, 1.914	
CO <sub>2</sub>	Ni <sub>2</sub> -top	η <sup>2</sup> (C, O)	-2.18	1.277, 1.213	1.893	1.919
H <sub>2</sub> O	Ni-top	η <sup>1</sup> (O)	-1.20		2.015	
OH	Ni <sub>2</sub> -bridge	η <sup>1</sup> (O)	-4.54		1.934, 1.939	
H	O-top	η <sup>1</sup> (H)	-1.19			

Table S2: Reaction energies (ΔE), activation energy barriers (E<sub>a</sub>) for the elementary steps involved in the methanol oxidation on NiO(100)

Reactions	ΔE (eV)	E <sub>a</sub> (eV)
CH <sub>3</sub> OH → CH <sub>2</sub> OH + H	-0.05	0.86
CH <sub>3</sub> OH → CH <sub>3</sub> O + H	-0.27	0.54
CH <sub>3</sub> O → CH <sub>2</sub> O + H	-1.27	0.90
CH <sub>2</sub> O → CHO + H	-1.05	0.84
CHO → CO + H	-1.24	0.73
CHO + OH → HCOOH	+0.19	0.58
HCOOH → COOH + H	-0.79	0.72
COOH → CO <sub>2</sub> + 2H	-0.31	0.68
HCOOH → HCOO + H	-1.21	1.16
HCOO → CO <sub>2</sub> + 2H	+1.13	0.97